

Trifluoromethyl Chloroformate, $\text{ClC}(\text{O})\text{OCF}_3$: Structure, Conformation, and Vibrational Analysis Studied by Experimental and Theoretical Methods[†]

Mauricio F. Erben,[‡] Carlos O. Della Védova,^{*,‡,§} Roland Boese,^{*,||} Helge Willner,^{*,⊥,#} and Heinz Oberhammer^{*,*}

CEQUINOR (CONICET-UNLP), Departamento de Química, Facultad de Ciencias Exactas, Universidad Nacional de La Plata, 47 esq. 115 (1900) La Plata, República Argentina, Laboratorio de Servicios a la Industria y al Sistema Científico (UNLP-CIC-CONICET), Departamento de Química, Facultad de Ciencias Exactas, Universidad Nacional de La Plata, 47 esq. 115 (1900) La Plata, República Argentina, Institut für Anorganische Chemie, Universität GH Essen, Universitätsstr. 5-7, D-45117 Essen, Germany, Fakultät 4, Anorganische Chemie, Universität Duisburg, Lotharstrasse 1, 47048 Duisburg, Germany, and Institut für Physikalische und Theoretische Chemie, Universität Tübingen, D-72076 Tübingen, Germany

Received: October 3, 2003; In Final Form: November 20, 2003

The gas phase conformational properties and geometric structure of trifluoromethyl chloroformate, $\text{ClC}(\text{O})\text{OCF}_3$, have been studied by vibrational spectroscopy (IR (gas), IR (matrix), and Raman (liquid)), gas electron diffraction (GED), and quantum chemical calculation (HF, B3LYP and MP2 methods with 6-311G* basis sets). The molecule exhibits only one form having C_s symmetry with synperiplanar orientation of the O–C single bond relative to the C=O double bond. If heated Ar: $\text{ClC}(\text{O})\text{OCF}_3$ mixtures are deposited as a matrix at 14 K, bands appear in the IR spectra which are assigned to the anti form. At room temperature, the contribution of the anti rotamer is estimated to be less than 1%. This high energy conformer is not observed in the GED experiment. The structure of solid $\text{ClC}(\text{O})\text{OCF}_3$ was determined by X-ray diffraction analysis from crystals obtained at low temperature, using a miniature zone melting procedure. The molecule crystallizes forming a dimeric structure belonging to the monoclinic crystal system and adopts the $P2_1/n$ spatial group. Furthermore, we report the structure of the similar molecule trifluoroacetyl chloride, $\text{CF}_3\text{C}(\text{O})\text{Cl}$, in its crystalline phase by using the same method.

Introduction

Perfluoroalkyl haloformates ($\text{XC}(\text{O})\text{OR}_F$, X = halogen) have been known since 1965 when Anderson et al.¹ reported the synthesis of $\text{FC}(\text{O})\text{OCF}_3$ by dimerization of carbonyl fluoride. Later, Aymonino² reported a more efficient synthesis of $\text{FC}(\text{O})\text{OCF}_3$ by photolysis of a mixture of CF_3OF and CO. At the same time, the synthesis of perhaloalkyl hypochlorites (R_FOCl) and the reaction of these compounds with carbon monoxide to give perfluoroalkyl chloroformates $\text{ClC}(\text{O})\text{OR}_F$ with $\text{R}_F = \text{CF}_3$, CF_2CF_3 , $i\text{-C}_3\text{F}_7$, and SF_5 were reported by several groups.^{3,4} Chloroformates are useful as catalysts for the polymerization of unsaturated compounds and in the preparation of polycarbonates, polyesters, and formaldehyde polymers.⁵

Although structural,⁶ spectroscopic (IR, Raman, mass spectra, and ¹⁹F NMR),⁷ and kinetic properties⁸ of fluoroformates have attracted great attention, little is known about perfluoroalkyl chloroformates. In a recent work, the preference for the syn conformation for $\text{FC}(\text{O})\text{OCF}_3$ was established, both experimen-

tally by gas electron diffraction (GED) experiments and theoretically at the MP2 and B3LYP methods. A contribution of about 4% for the anti form ($\Delta H = H_{\text{anti}} - H_{\text{syn}} = 1.97(5)$ kcal/mol) was deduced from IR (matrix) spectra.⁶

A similar conformational behavior was recently found for trifluoromethyl formate $\text{HC}(\text{O})\text{OCF}_3$. Wallington et al.⁹ have reported that the atmospheric oxidation of fluorinated ethers, specifically of CF_3OCH_3 (E143a), produces trifluoromethyl formate. The syn conformer of $\text{HC}(\text{O})\text{OCF}_3$ was calculated (MP2/TZ2P) to be about 1 kcal/mol more stable than the anti form.¹⁰ The presence of the less stable anti form at room temperature was detected experimentally by examination of the carbonylic stretching region in the IR (gas) spectrum.⁹

In continuation of studies for $\text{XC}(\text{O})\text{OCF}_3$ molecules, we present in this work an experimental investigation of the structure and vibrational properties of $\text{ClC}(\text{O})\text{OCF}_3$ which includes the use of GED technique, IR (gas) and IR (matrix) spectroscopy, and the Raman spectrum of liquid $\text{ClC}(\text{O})\text{OCF}_3$. In principle, $\text{ClC}(\text{O})\text{OCF}_3$ can possess two conformations with syn and anti orientation of the O–C single bond respect to the C=O double bond (Chart 1). The crystal structure of the title compound was also obtained by using the low-temperature X-ray diffraction method. The crystal structure of the similar molecule $\text{CF}_3\text{C}(\text{O})\text{Cl}$ was also determined by the same technique. The experimental data were supplemented by using ab initio (HF and MP2) and DFT (B3LYP) quantum chemical calculations.

[†] Dedicated to Prof. Dr. Pedro J. Aymonino on occasion of his 75th birthday on July 20, 2003.

* To whom correspondence should be addressed. E-mail: carlosdv@quimica.unlp.edu.ar, heinz.oberhammer@uni-tuebingen.de, and willner@uni-duisburg.de. E-mail: boese@structchem.uni-essen.de.

[‡] CEQUINOR (CONICET-UNLP).

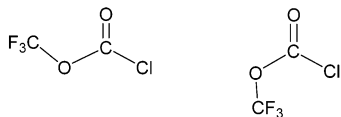
[§] UNLP-CIC-CONICET.

^{||} Universität GH Essen.

[⊥] Universität Duisburg.

[#] Present address: FB9, Anorganische Chemie, Universität Wuppertal, Gausstr. 20, D-42097 Wuppertal, Germany.

* Universität Tübingen.

CHART 1. Representation of the syn (Left) and anti (Right) Conformers of $\text{ClC}(\text{O})\text{OCF}_3$.**Experimental Section**

Synthesis. $\text{ClC}(\text{O})\text{OCF}_3$ was synthesized by reaction of CF_3OCl with CO according to the method reported by Young et al.³ Conventional vacuum techniques were used to condense trifluoromethyl hypochlorite into a 60 mL stainless steel cylinder. This was followed by the addition of excess carbon monoxide at -196°C . The mixture was then allowed to warm to -20°C and remain at that temperature for about 10 h. After this time, the products were separated by vacuum fractionation. The yield of chloroformate was nearly quantitative. CF_3OCl was synthesized by reaction of carbonyl fluoride and chlorine monofluoride in the presence of cesium fluoride (p. a. Fluka) catalyst at -20°C . Fractionation of the reaction products through traps at -100 , -140 , and -196°C yields pure CF_3OCl which is retained as a pale yellow liquid in the -140 trap.¹¹ $\text{CF}_3\text{C}(\text{O})\text{Cl}$ was synthesized by reaction of trifluoroacetic acid with pentachlorophosphorane according to the usual method.¹² The compounds were purified by trap-to-trap distillation and the final purity ($>98\%$) was checked by IR and ^{19}F NMR spectroscopy. CO (95.5%, Linde, Munich, Germany) and F_2CO (Messer Griesheim) were obtained from commercial sources and used without further purification.

General Procedure. Volatile materials were manipulated in a glass vacuum-line equipped with two capacitance pressure gauges (221 AHS-1000 and 221 AHS-10, MKS Baratron, Burlington, MA), three U-traps, and valves with PTFE systems (Young, London, U.K.). The vacuum line was connected to an IR cell (optical path length 200 mm, Si windows 0.5 mm thick) contained in the sample compartment of an FTIR instrument (Impact 400D, Nicolet, Madison, WI). This allowed us to observe the purification processes and to follow the course of the reactions. The pure compound was stored in flame-sealed glass ampules under liquid nitrogen in a long-term Dewar vessel. The ampules were opened with an ampule key¹³ on the vacuum line, an appropriated amount was taken out for the experiments, and then they were flame-sealed again.

Preparation of Matrixes. In a stainless steel vacuum line (1.1 L volume), a small amount of $\text{ClC}(\text{O})\text{OCF}_3$ (ca. 0.05 mmol) was mixed with an 1:1000 excess of Ar. This mixture was passed into a stainless steel capillary, in 20–60 min, and a heated quartz nozzle, which was placed directly in front of the matrix support at 14 K. For the pyrolysis of $\text{ClC}(\text{O})\text{OCF}_3$, the nozzle temperature was varied between room temperature and 565 K. Photolysis experiments on the matrixes were undertaken in the UV region by using a high-pressure mercury lamp (TQ 150, Heraeus, Hanau, Germany) in combination with a water-cooled cut off filter (Schatt, Mainz, Germany). Details of the matrix apparatus have been given elsewhere.¹⁴ IR (matrix) spectra were recorded on a IFS66v/S FT spectrometer (Bruker, Karlsruhe, Germany) in the reflectance mode with a transfer optic. A DTGS detector with a KBr/Ge beam splitter in the region $\nu = 4000\text{--}400\text{ cm}^{-1}$ was used. In this region, 64 scans were co-added for each spectrum by means of apodized resolution of 1 cm^{-1} .

Instrumentation. (A) *Gas Electron Diffraction.* Electron diffraction intensities were recorded with a Gasdiffraktograph KD-G2¹⁵ at 25 and 50 cm nozzle-to-plate distances and with

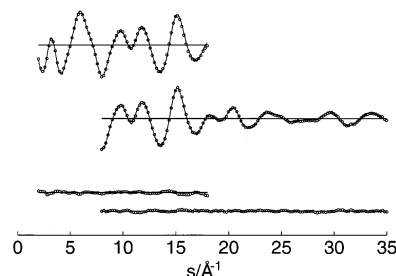


Figure 1. Experimental (dots) and calculated (full line) molecular scattering intensities and differences for $\text{ClC}(\text{O})\text{OCF}_3$.

an accelerating voltage of about 60 kV. The sample was cooled to -60°C , and the inlet system and nozzle were at room temperature. The photographic plates were analyzed with the usual methods¹⁶ and averaged molecular intensities in the s -ranges 2–18 and 8–35 \AA^{-1} ($s = (4\pi/\lambda) \sin \vartheta/2$, λ = electron wavelength, ϑ = scattering angle) are shown in Figure 1.

(B) *X-ray Diffraction at Low Temperature.* An appropriate crystal of ca. 0.3 mm diameter of $\text{ClC}(\text{O})\text{OCF}_3$ and $\text{CF}_3\text{C}(\text{O})\text{Cl}$ was obtained on the diffractometer at a temperature of 138 K with a miniature zone melting procedure using focused infrared laser radiation.^{17,18} The diffraction intensities were measured at low temperature on a Nicolet R3m/V four circle diffractometer. Intensities were collected with graphite-monochromatized $\text{Mo K}\alpha$ radiation using the ω -scan technique. The crystallographic data, conditions, and some features of the structure are listed in Table 1. The structure was solved by Patterson syntheses and refined by full-matrix least-squares method on F, with the SHELXTL-Plus program.¹⁹ All atoms were assigned to anisotropic thermal parameters. Atomic coordinates and equivalent isotropic displacement coefficients and anisotropic displacement parameters ($\text{\AA}^2 \times 10^3$) for $\text{ClC}(\text{O})\text{OCF}_3$ are given as Supporting Information. Crystal structure data have been deposited at the Cambridge Crystallographic Data Centre (CCDC). Enquiries for data can be direct to: Cambridge Crystallographic Data Centre, 12 Union Road, Cambridge, UK, CB2 1EZ or (e-mail) deposit@ccdc.cam.ac.uk or (fax) +44 (0) 1223 336033. Any request to the Cambridge Crystallographic Data Centre for this material should quote the full literature citation and the reference numbers 219229 and 220881 for $\text{ClC}(\text{O})\text{OCF}_3$ and $\text{CF}_3\text{C}(\text{O})\text{Cl}$, respectively.

(C) *Vibrational Spectroscopy.* Gas-phase infrared spectra were recorded with a resolution of 1 cm^{-1} in the range 4000–400 cm^{-1} on the FTIR instrument Bruker IFS 66v. FT-Raman spectra of liquid $\text{ClC}(\text{O})\text{OCF}_3$ were recorded with a Bruker RFS 100/S FT Raman spectrometer. The sample in a o.d. 4 mm glass tube was excited with 500 mW of a 1064 nm Nd:YAG laser (ADLAS, DPY 301, Lübeck, Germany).

(D) *NMR Spectroscopy.* The ^{19}F and ^{13}C NMR spectra of the neat liquid sample were recorded with a Bruker MSL 200 spectrometer and a $^{19}\text{F}/^1\text{H}$ dual head (for ^{19}F) or a multinuclear probe head (for ^{13}C) operating at 188.31 and 50.33 MHz, respectively. For each ^{19}F NMR spectrum, four scans were accumulated in a 64-kB memory, with a delay time of 2.2 s between scans. For the ^{13}C NMR spectrum, 132 scans of the same sample were recorded with a delay time of 60 s. Low-temperature measurements (-70°C) were carried out by using a Bruker variable-temperature controller with a copper–constant thermocouple.

Results

Quantum Chemical Calculations. All calculations were performed with the Gaussian 98 software package.²⁰ The

TABLE 1: Crystal Data and Structure Refinement for ClC(O)OCF₃^a

empirical formula	C ₂ ClF ₃ O ₂	cell measurement reflections used	2189
formula weight	148.47 Da	cell measurement theta min/max	2.504° to 28.324°
density (calculated)	1.986 g cm ⁻³	diffractometer measurement method	data collection in omega at 0.3° scan width one run with 740 frames, phi = 0°, chi = 0°
F(000)	576	theta range for data collection	2.54° to 28.32°
temperature	138(2) K	completeness to theta = 28.31°	69.7%
crystal size	0.3 mm diameter	index ranges	-11 ← h ← 8, -6 ← k ← 6, -18 ← l ← 18
crystal color	colorless	absorption coefficient	0.741 mm ⁻¹
crystal description	cylindric	absorption correction details	Blessing, R. H. <i>Acta Cryst.</i> 1995 , A51, 33-38
wavelength	0.71073 Å	max./min. transmission	1.00/0.94
crystal system	monoclinic	R(merge) before/after correction	0.0372/0.0217
space group	P2 ₁ /n	weighting details	w = 1/(σ ² (Fo ²) + (0.0472*P) ² + 0.4756*P) where P = (Fo ² + 2Fc ²)/3
unit cell dimensions	a = 8.917(3) Å b = 8.085(2) Å c = 13.960(4) Å β = 99.260(7)°	final R indices [I > 2σ(I)]	R1 = 0.0424, wR2 = 0.1157
volume	993.3(5) Å ³	R indices (all data)	R1 = 0.0559, wR2 = 0.1445
Z	8	largest diff. peak and hole	0.301 and -0.347 eÅ ⁻³
reflections collected	3621	data/restraints/parameters	1357/0/146
independent reflections	1721 [R(int) = 0.0158]	goodness-of-fit on F ²	1.121

^a The crystallization was performed on the diffractometer at a temperature of 138 K with a miniature zone melting procedure using focused infrared-laser-radiation according to ref 18. Computing structure solution: Bruker AXS SHELXTL Vers. 5.10 DOS/WIN95/NT. Computing structure refinement: Bruker AXS SHELXTL Vers. 5.10 DOS/WIN95/NT. Diffractometer control software: Bruker AXS SMART Vers. 5.054 1997/98. Diffractometer measurement device: Siemens SMART CCD area detector system. Computing data reduction: Bruker AXS SAINT program Vers. 6.02^a. Computing absorption correction: Bruker AXS SADABS program multiscan V2.03. Refinement method: Full-matrix least-squares on F².

TABLE 2: Observed and Calculated Vibrational Data for ClC(O)OCF₃ (cm⁻¹)

IR ^a	experimental			calculated ^d		Δ ^e		mode symmetry/assign./approximately description of mode
	Raman ^b	Ar matrix ^c		syn	anti	Exptl.	Calcd	
		syn	anti					
3656 (0.5)								2 × ν ₁
2200 (0.4)								2 × ν ₄
1837 (34) ^f	1824 s	1829 (39)	1838	1902 (38)	1911 (82)	-9	-9	A'/ν ₁ /ν (C=O)
1771 (1.2)								ν ₄ + ν ₇
1286 (38)	1286 vw	1284 (36)	1280	1281 (31)	1276 (100)	4	5	A'/ν ₂ /ν _{as} (CF ₃)
1199 (24)	1193 vw	1196 (23)	1204	1174 (8)	1182 (97)	-8	-9	A'/ν ₃ /ν _s (CF ₃)
1106 (100)	1090 vw	1099 (100)	1113	1089 (100)	1103 (80)	-14	-14	A'/ν ₄ /ν _{as} (C-O-C)
879 (17)	867 vs	882 (15)	913	870 (11)	896 (37)	-31	-26	A'/ν ₅ /ν _s (C-O-C)
850 (3)				866 (5)	741 (9)			A'/ν ₆ /ν (C-Cl)
672 (13)	671 m	672 (13)		659 (7)	653 (4)			A'/ν ₇ /δ _s (CF ₃)
	576 s			570 (0.05)	531 (3)			A'/ν ₈ /δ _{as} (CF ₃)
	492 s			481 (0.5)	489 (0.6)			A'/ν ₉ /δ (O=C-O-C)
	382 w			378 (0.01)	406 (0.06)			A'/ν ₁₀ /ρ (CF ₃)
	296 s			287 (0.08)	311 (0.1)			A'/ν ₁₁ /ρ (F-C-O)
	168 w			164 (0.09)	163 (0.2)			A'/ν ₁₂ /δ (C-O-C)
1255 (37)		1248 (46)	1237	1243 (36)	1231 (76)	11	12	A''/ν ₁₃ /ν _{as} (CF ₃)
		683 (7)		684 (8)	656 (8)			A''/ν ₁₄ /ρ (Cl-C=O)
				601 (0.04)	606 (0.3)			A''/ν ₁₅ /δ _{as} (CF ₃)
	443 w			425 (0.02)	425 (0.02)			A''/ν ₁₆ /ρ (CF ₃)
	106 sh			99 (0.02)	93 (0.0008)			A''/ν ₁₇ /τ (O-C=OCl)
				63 (0.006)	35 (0.1)			A''/ν ₁₈ /τ (O-CF ₃)

^a Gas phase. In parentheses relative absorbance at band maximum. ^b Liquid, room temperature, band intensities: vs = very strong; s = strong; m = medium; w = weak; vw = very weak. ^c Band position at the most intensive matrix site. In parentheses relative integrated absorbance of the syn rotamer deposited with the spray on nozzle held at room temperature. The band position of the anti rotamer correspond to mixtures Ar/ClC(O)OCF₃ deposited on nozzle held at 565 K. ^d B3LYP(6-311G*). In parentheses relative band strength of syn rotamer; 100 ≡ 1101 km mol⁻¹ and anti rotamer; 100 ≡ 523.5 km mol⁻¹. ^e Wavenumber differences between the syn and anti conformers. ^f B-type band (see text).

molecular geometries were optimized to standard convergence criteria by using a DFT²¹ hybrid method with Becke's^{22,23} nonlocal three parameter exchange and the Lee, Young, and Parr²⁴ correction (B3LYP) and a triple split valence 6-311G* basis sets. Both conformers with C_s symmetry were found to be stable structures. The B3LYP/6-311G* method predicts the syn conformation to be lower in energy than the anti form by 3.98 kcal/mol. For comparison, calculations were also performed with the Hartree-Fock (HF) method and with the second-order perturbation theory from Møller and Plesset²⁵ (MP2) by using the same 6-311G* basis set. Both HF and MP2 calculations

predict the syn form to be more stable than the anti form by 5.66 and 5.13 kcal/mol, respectively.

The potential functions for internal rotation around the C(sp²)-O bond was derived with the B3LYP/6-311G* method, performing geometry optimizations for fixed δ(C=O-O-C) dihedral angles. Calculated geometrical parameters, vibrational frequencies and IR intensities are compared to experimental values in the respective tables.

NMR Spectra. In the ¹⁹F NMR spectrum of a ClC(O)OCF₃ neat sample at -70 °C, one signal at -60.2 ppm was observed. This observation agrees with the reported literature value³ of

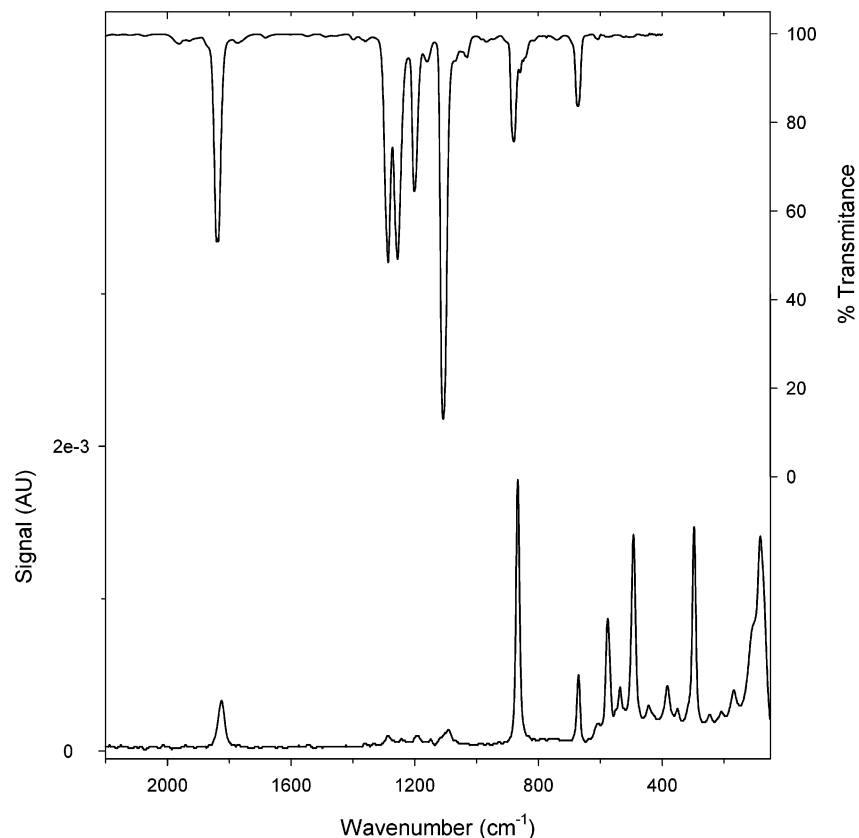


Figure 2. Upper trace: IR (gas) spectrum of ClC(O)OCF_3 (10 mbar at 20 cm optical path length and 300 K). Lower trace: Raman (liquid) spectrum of ClC(O)OCF_3 .

−61 ppm. The coupling constants $^1J_{\text{CF}}$ and $^3J_{\text{CF}}$ were also determined from the ^{13}C satellites to be 270.6 and 1.9 Hz, respectively. The ^{13}C NMR spectrum of the same sample at −70 °C has been measured for the first time and shows two quartets at 118.6 and 143.4 ppm with the same J_{CF} coupling constants as in the ^{19}F NMR spectrum. All NMR data agree with reported values for similar compounds containing the $\text{CF}_3\text{-OC(O)}$ moiety.²⁶

Vibrational Analysis and Matrix Infrared Spectra. To our knowledge, no detailed vibrational study on ClC(O)OCF_3 has been performed. Although the IR (gas) spectra was reported previously,^{3,4} it has been only used as purity criteria, without assignments of the bands.

The observed band positions in the IR (gas and matrix) and Raman spectra together with calculated wavenumbers (B3LYP/6-311G*) are collected in Table 2. Figure 2 shows the IR (gas) Raman (liquid) spectra of ClC(O)OCF_3 . All 18 normal modes of vibration in ClC(O)OCF_3 are active in the IR and Raman spectrum and can be classified as 12 A' in-plane modes and 6 A'' out-of-plane modes in the C_s symmetry group. The agreement between calculated and observed IR frequencies is satisfying and is illustrated in Figure 3 by comparison of the experimental spectrum obtained in an Ar matrix at 14 K with the calculated (B3LYP) spectrum.

The assignment of the observed bands is performed by comparison with the calculated spectra, and the approximate description of modes is based on the calculated displacement vectors for the fundamentals as well as on comparison with spectra of related molecules, mainly FC(O)OCF_3 ⁶ and ClC(O)OCH_3 .^{27,28}

The most intense gas-phase IR band at 1106 cm^{-1} was assigned to the C—O—C antisymmetric stretching. The spectrum also shows three strong absorptions between 1190 and 1300

cm^{-1} assigned to CF_3 stretching modes, similar to those found for FC(O)OCF_3 .²⁹ The characteristic $\nu_{\text{C-Cl}}$ stretching mode appears as a low intensity band at 850 cm^{-1} .

An important feature of the infrared spectrum is the $\nu_{\text{C=O}}$ stretching band at 1837 cm^{-1} shifted to a lower frequency from that of FC(O)OCF_3 (1906 cm^{-1}).² This is expected from the higher electronegativity of the F atom compared to that of the Cl atom.⁴ The band contour of the $\nu_{\text{C=O}}$ stretching mode in the IR (gas) spectrum (Figure 4) can be described as B-type. This demonstrates the presence of the syn conformer, for which the carbonyl oscillator is almost parallel to the B axis.

The Raman (liquid) spectra shows a strong signal at 867 cm^{-1} due to the C—O—C symmetric stretching mode and two other less intense signals at 576 and 492 cm^{-1} due to the CF_3 antisymmetric and to the O=C—Cl deformations, respectively. The carbonylic stretching mode appears in the Raman spectrum at 1824 cm^{-1} as a strong intensity signal.

If an Ar/ ClC(O)OCF_3 mixture passed through a heated spray-on nozzle and the heated mixture is subsequently deposited as a matrix, new bands appear in the IR spectra. These were assigned to the high energy conformer. Figure 5, shows the 1300–1180 cm^{-1} region deposited at 300 and 565 K. The CF_3 stretching bands of the anti form are clearly observed. Six modes belonging to the anti form, which were computed to be the most intense ones, were assigned. The band positions of the anti form isolated in Ar matrix at 14 K are listed in Table 2. The observed absolute wavenumber differences as well as the sign of the shift between the syn and anti form are in perfect agreement with the calculated (B3LYP/6-311G*) frequencies for both conformers. With the nozzle held at room temperature, no bands of this high-energy conformer could be detected in the IR (matrix) spectrum. Thus,³⁰ the presence of the less stable anti form for ClC(O)OCF_3 at room temperature could be excluded.

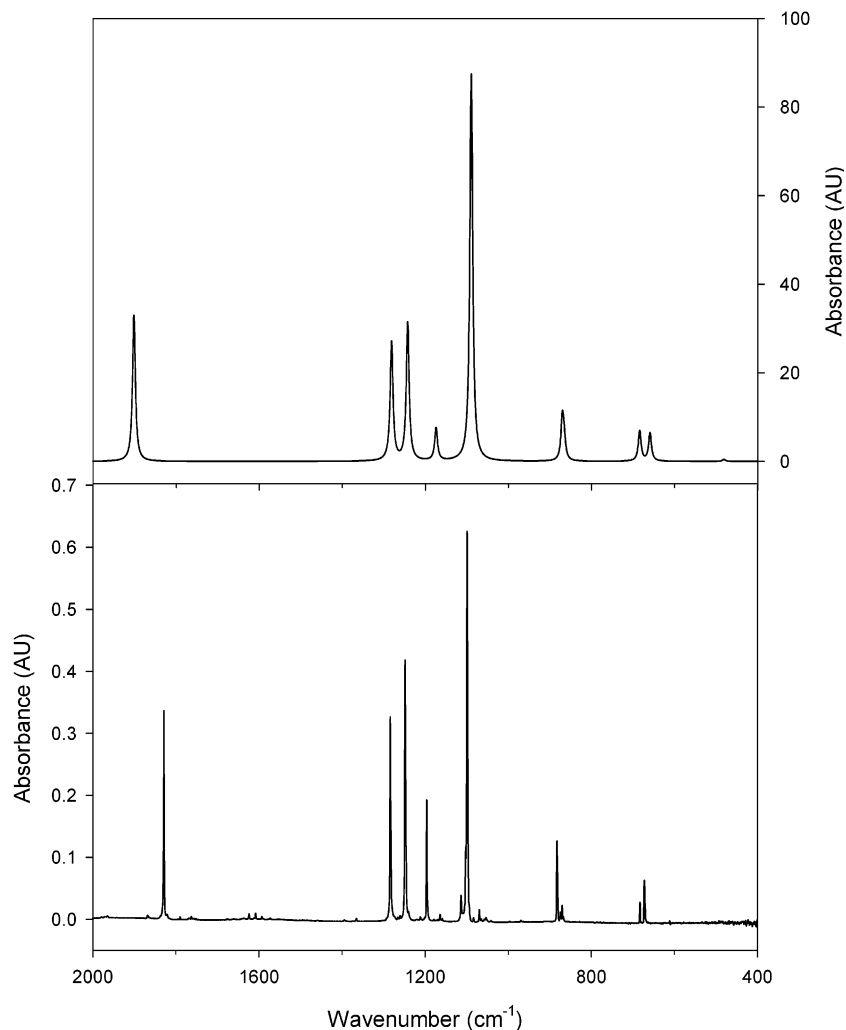


Figure 3. Lower trace: Ar matrix IR spectrum of ClC(O)OCF₃ at 300 K. Upper trace: simulated infrared spectrum for syn ClC(O)OCF₃ from B3LYP/6-311G* calculation.

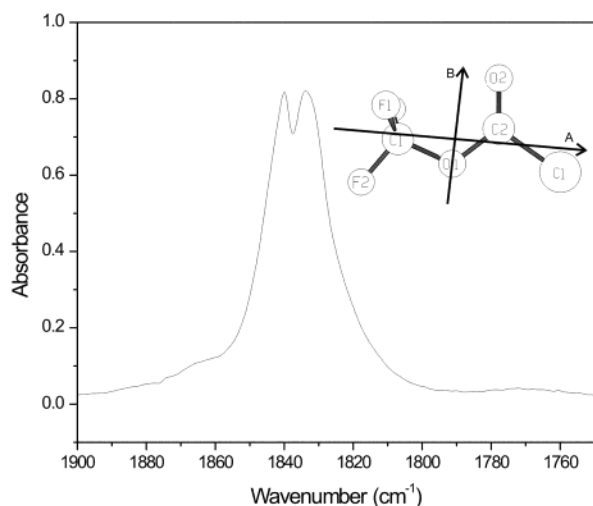


Figure 4. Principal axes (A and B) for the syn conformer of ClC(O)OCF₃ (the C axis is perpendicular to the symmetry molecular plane) and gas IR carbonylic stretching $\nu_{C=O}$ band of ClC(O)OCF₃ at 2 mbar.

The thermal decomposition of alkyl chloroformates ClC(O)OR, R = alkyl group, to give RCl and CO₂ is considered to be an example for the S_N1 mechanism.³¹ ClC(O)OCH₃ shows such decomposition at 240 °C with a rate constant of $0.533 (22) \times 10^{-5} \text{ s}^{-1}$.³² Gaseous ClC(O)OCCl₃, however, decomposes at 300 °C to phosgene, Cl₂CO, and not to the expected

products CCl₄ and CO₂. This has been explained by low stability of the S_N1 transition state for R = CCl₃.³³ In agreement with this trend, ClC(O)OCF₃ shows a high thermal stability, and even at a temperature as high as 565 K, no decomposition products could be observed in the IR (matrix) spectra. Similarly, a high stability was observed toward UV-vis broad band irradiation. After 90 min of irradiation, no decomposition products could be detected by analysis of the IR spectra.

Structure Analyses. (a) *Gas-Phase Structure.* The radial distribution function (RDF) which was derived by Fourier transformation of the modified molecular intensities (Figure 6) can be reproduced satisfactorily only with syn orientation of the O-C bond relative to the C=O bond. This is in agreement with the predictions from the quantum chemical calculations. An r_α structure was refined by least-squares fitting of the molecular intensities. The vibrational corrections $\Delta r = r_\alpha - r_a$ and vibrational amplitudes were calculated from a theoretical force field (B3LYP/6-311G*) with the method of Sipachev.³⁴ A planar model with C_s overall symmetry and local C_{3v} symmetry for the CF₃ group was assumed. A mean value of the C-O single bonds was refined, and the difference $\Delta CO = (C1-O1) - (C2-O1)$ was constrained to the calculated (MP2) value. Vibrational amplitudes, which caused either large correlations between geometric parameters or which were badly determined in the GED experiment, were set to calculated values. With these assumptions nine geometric parameters p_1

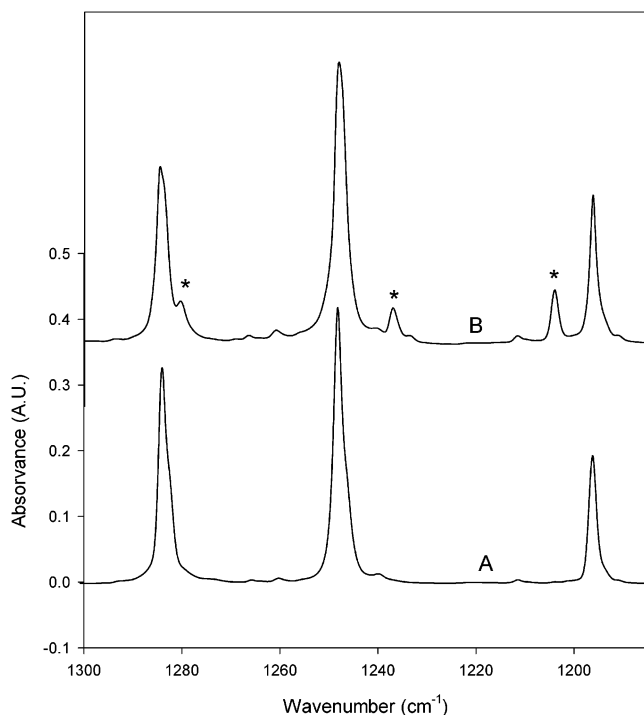


Figure 5. IR (matrix) spectrum in the 1300–1180 cm^{-1} region of ClC(O)OCF_3 deposited at nozzle temperatures of 300 (A), and 565 K (B). The asterisks indicate bands belonging to the anti form.

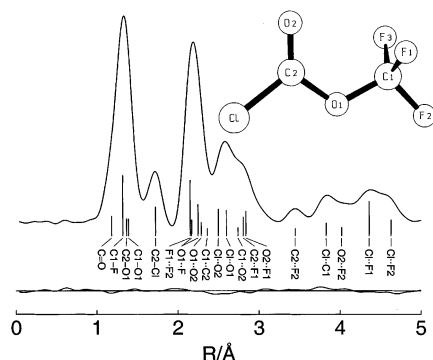


Figure 6. Calculated radial distribution function for syn ClC(O)OCF_3 and experimental and difference curves ($\text{RDF}(\text{exp})-\text{RDF}(\text{calc})$). Interatomic distances of the syn structure are indicated by vertical bars.

to p_9 and p_{10} vibrational amplitudes l_1 to l_{10} were refined simultaneously. The following correlation coefficients had values larger than $|0.6|$: $p_2/p_3 = -0.72$, $p_3/p_8 = 0.84$, $p_2/l_1 = -0.84$, $p_5/l_6 = 0.72$ and $l_5/l_6 = 0.83$. The geometric parameters derived in this analysis are listed in Table 3 together with the X-ray diffraction results and the calculated values. Vibrational amplitudes are given together with the calculated values and with vibrational corrections in Table 4.

(b) *Crystal Structures.* Because simple perfluoromethyl or perfluoromethoxy carbonyl compounds are liquids or gases at ambient temperatures, little is known about their structures in the solid state. Only with the development of special crystallization techniques applicable to compounds which are liquids or gases at room temperature, it has been possible to extend detailed structural studies to the crystalline state. To compare structural parameters for these kinds of molecules measured in gas and solid phases with those obtained by quantum chemical calculations, a study was performed for the structurally well-known and related $\text{CF}_3\text{C(O)Cl}$ molecule. The results are summarized in Table 5. X-ray parameters for $\text{CF}_3\text{C(O)Cl}$ are very similar to those reported for the molecule in the gas phase,³⁵

TABLE 3: Experimental and Calculated Geometric Parameters for ClC(O)OCF_3^a

	GED(r_α) ^b		X-ray ^c	MP2 ^d	B3LYP ^d
C=O	1.185(5)	p_1	1.164(4)	1.186	1.178
(C–O) _{mean}	1.383(6)	p_2	1.377(4)	1.379	1.380
C2–O1	1.371(6)		1.367(4)	1.367	1.364
C1–O1	1.394(6)		1.386(3)	1.390	1.396
(C–F) _{mean}	1.322(3)	p_3	1.310(4)	1.320	1.328
C2–Cl	1.726(4)	p_4	1.716(3)	1.735	1.761
O2=C2–O1	126.6(8)	p_5	126.9(3)	127.2	127.6
O2=C2–Cl	125.6(5)		125.3(2)	125.4	125.0
Cl–C2–O1	107.7(7)	p_6	107.8(2)	107.4	107.5
C1–O2–C2	117.6(6)	p_7	116.9(3)	116.5	118.2
(F–C–F) _{mean}	109.1(5)	p_8	109.1(3)	109.2	109.3
tilt (CF ₃) ^e	4.0(7)	p_9	3.9(5)	3.9	3.8

^a For atom numbering, see Figure 6. ^b r_α parameters in Å and deg. Uncertainties are 3σ values. ^c Mean values of the two molecules in the unit cell, uncertainties are σ values. ^d 6-311G* basis sets. ^e Tilt angle between C₃ axis of CF₃ group and O–C bond direction, away from C=O bond.

TABLE 4: Interatomic Distances, Experimental and Calculated (MP2/6-311G*) Vibrational Amplitudes, and Corrections^a

	distance	ampl. (GED) ^b		ampl. (MP2)	$\Delta r = r_\alpha - r_a$
C=O	1.18	0.036 ^c		0.036	0.0011
C1–F	1.32	0.047(4)	l_1	0.044	0.0014
C–O	1.37–1.39	0.047 ^c		0.047	0.0016
F1...F2	2.15	0.052(5)	l_2	0.048	0.0013
C2–Cl	1.73	0.055(3)	l_3	0.055	0.0035
O1...F	2.17–2.25	0.058 ^c		0.058	0.0037
O1...O2	2.29	0.052 ^c		0.052	0.0040
C1...C2	2.36	0.069(10)	l_4	0.061	0.0031
Cl...O2	2.50	0.066(15)	l_5	0.059	0.0043
Cl...O1	2.60	0.056(12)	l_6	0.055	0.0048
C1...O2	2.74	0.088 ^c		0.088	–0.0037
C2...F1	2.81	0.091(15)	l_7	0.110	0.0040
O2...F1	2.84	0.192(36)	l_8	0.164	–0.0039
C2...F2	3.45	0.069(10)	l_4	0.061	0.0118
Cl...C1	3.83	0.069(10)	l_4	0.063	0.0178
O2...F2	4.02	0.095(16)	l_9	0.082	0.0078
Cl...F2	4.36	0.134(13)	l_{10}	0.137	0.0225
Cl...F1	4.63	0.095(16)	l_9	0.082	0.0286

^a Values in Å. For atom numbering, see Figure 6. ^b Uncertainties are 3σ values. ^c Not refined.

TABLE 5: GED, X-ray, and Calculated Geometric Parameters for $\text{CF}_3\text{C(O)Cl}^a$

	GED ^{b,c}	X-ray	HF/6-31G ^{*b}	B3LYP/6-311G [*]	MP2/6-311G [*]
C–Cl	1.742(4)	1.724	1.741	1.782	1.752
C=O	1.186(4)	1.171	1.164	1.177	1.190
C–C	1.533(6)	1.535	1.519	1.555	1.547
C–F(av)	1.329(2)	1.313	1.340	1.336	1.330
Cl–C=O	123.1(7)	124.49	123.7	123.8	124.4
C–C–Cl	110.9(5)	112.85	113.5	112.3	112.1
C–C=O	126.2(8)	122.62	122.8	123.9	123.6
F–C–F(av)	108.7(2)	108.22	109.0	109.0	109.0
$\delta(\text{FC–C(O)})$	0.0	15.0	0.0	0.0	0.0

^a Bond lengths in Å, bond angles in degrees. ^b Reference 35. ^c C_s symmetry.

except for the orientation of the CF₃ group. Whereas an exactly eclipsed orientation of one C–F bond ($\delta(\text{FC–C(O)}) = 0^\circ$) was assumed in the GED analysis, a value of 15° was derived for this dihedral angle from X-ray data. This appears to be a distortion due to packing effects, because the calculations confirm the assumption made in the GED analysis. Unit cell parameters for $\text{CF}_3\text{C(O)Cl}$ are $a = 5.7258(9)$, $b = 5.3673(10)$, $c = 14.796(2)$, $\beta = 99.362(12)$ with the spatial group $P2_1/n$.

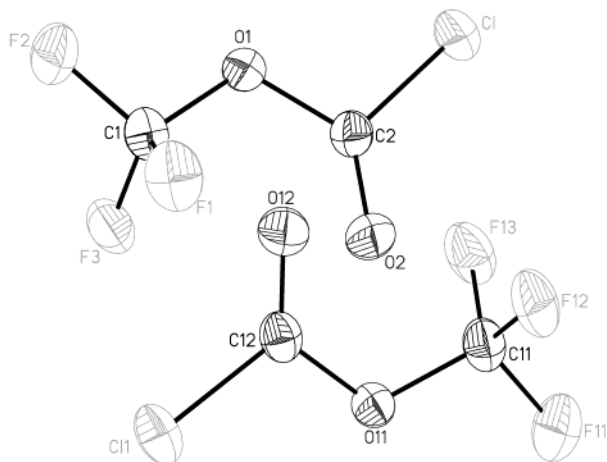


Figure 7. Dimeric single-crystal structure for $\text{ClC}(\text{O})\text{OCF}_3$.

All methods reproduce the experimental bond lengths and bond angles reasonably well with the exception of the C–Cl bond, which is predicted too long by the B3LYP method.

$\text{ClC}(\text{O})\text{OCF}_3$ crystallizes in the monoclinic crystal system ($P2_1/n$ spatial group) with unit cell dimensions of $a = 8.917(3)$ Å, $b = 0.8085(2)$ Å, $c = 13.960(4)$ Å and $\alpha = \gamma = 90^\circ$ and $\beta = 99.260(7)^\circ$ (for the whole crystallographic information see Table 1). The packing is formed by dimers. Their molecules are displaced by each others with the approximate position of the $\text{ClC}(\text{O})$ group of one molecule in front of the C–O–C group of the other one as shown in Figure 7. Both molecules in the dimer have similar geometrical parameters. The differences are within the experimental uncertainties, except for the C=O bond lengths which differ by 0.009 Å and some parameters in the CF_3 group.

The presence of planar dimeric units in the crystal raises the question about intermolecular interactions. Quantum chemical calculations at the B3LYP/6-311G* level result in a stabilization energy of $\Delta E = -1.63$ kcal/mol for such a dimer. This interaction energy was calculated with the corrections proposed by Nagy et al.³⁶ and Boys and Benardi.³⁷ The presence of similar intermolecular interactions in the liquid phase is indicated by the Trouton's constant (23.2 cal/K mol).³ This value is slightly higher than that for nonassociated liquids (ca. 20 cal/K mol).

Discussion

According to the GED analysis and quantum chemical calculations, gaseous $\text{ClC}(\text{O})\text{OCF}_3$ exists in a single conformation at room temperature, with the synperiplanar orientation of the O–C single bond relative to the C=O double bond. According to the Figure 6 and Table 4, the $\text{F2}\cdots\text{O2}$ distance (4.02 Å) is clearly longer than the $\text{F1}\cdots\text{O2}$ distance (2.84 Å). It means that C–F bonds of the CF_3 group stagger the C=O bond. From IR (matrix) spectra, the contribution of the less stable anti form at room temperature is estimated to be less than 1%. In methyl chloroformate, $\text{ClC}(\text{O})\text{OCH}_3$, the preference of the syn orientation of the O–C single bond relative to the C=O double bond has been well established by microwave, Raman, and far infrared spectra.³⁸ Similar conformational properties were reported for trifluoromethyl fluoroformate, $\text{FC}(\text{O})\text{OCF}_3$, in which the syn form is preferred and a contribution of 4% of the anti form has been derived by IR (matrix) spectra.⁶ Figure 8 shows the calculated (B3LYP/6-311G*) potential curves for internal rotation around the C(sp²)-O bond for trifluoromethyl haloformates ($\text{XC}(\text{O})\text{OCF}_3$, X = F, Cl, and Br). According to these calculations, the energy difference

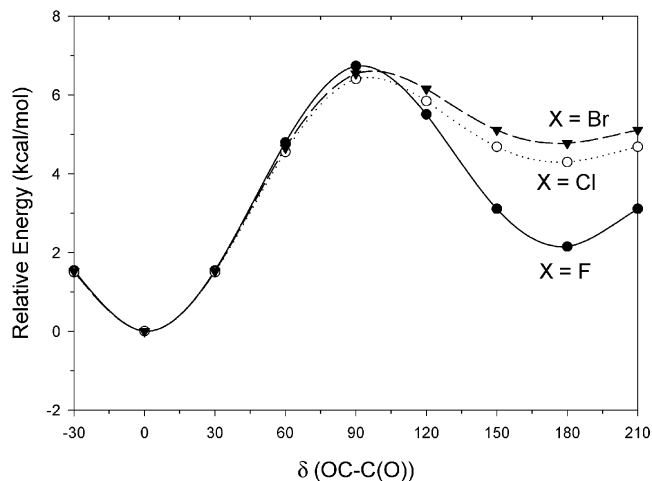


Figure 8. Potential energy curve for $\text{XC}(\text{O})\text{OCF}_3$ (X = F, Cl, and Br) as a function of the $\delta(\text{OC}-\text{C}(\text{O}))$ dihedral angle calculated with the B3LYP/6-311G* approximation.

between syn and anti forms is lowered from 4.8 and 4.3 kcal/mol in the bromo and chloro derivatives, respectively, to 2.1 kcal/mol in $\text{FC}(\text{O})\text{OCF}_3$. The barrier to internal rotation of about 6.6 kcal/mol, however, is similar for the three molecules. Attempts to rationalize this trend on the basis of a natural bond orbital (NBO)³⁹ analysis were unsuccessful. This indicates that interactions other than donor/acceptor electronic interactions, such as steric repulsion between the CF_3 group and the X atom, must play an important role. This destabilizes the anti conformer with increasing size of the X atom.

It should also be mentioned that in the closely related trifluoromethyl chlorothioformate, $\text{ClC}(\text{O})\text{SCF}_3$, GED and IR analyses agree with the presence of only the syn conformer at room temperature. The theoretical energy difference ΔE was calculated to be 3.7 kcal/mol with the MP2/6-31G* and 3.0 kcal/mol at the BPW91/6-31G* method.⁴⁰

Geometrical parameters measured for $\text{ClC}(\text{O})\text{OCF}_3$ are in close agreement with those values reported for equivalent parameters in $\text{FC}(\text{O})\text{OCF}_3$ ⁶ and in $\text{ClC}(\text{O})\text{OCH}_3$.³⁸ Quantum chemical calculations at the MP2/6-311G* level reproduce the gas-phase geometrical parameters within the experimental error, except for the C1–O2–C2 bond angle, which is calculated 1.1 degree smaller than that measured in the gas phase. The geometrical parameters measured in the crystalline phase are similar to those obtained in the gas phase. Differences are observed in the C=O and C–Cl bond lengths which are 0.02 and 0.01 Å shorter in the crystal.

Acknowledgment. The authors thank the ANPCYT-DAAD for the German-Argentinean cooperation Awards (PROALAR). They also thank to the Volkswagen Foundation for generous support of this work. M.F.E. and C.O.D.V. thank the Consejo Nacional de Investigaciones Científicas y Técnicas (CONICET), the Fundación Antorchas, and the Comisión de Investigaciones Científicas de la Provincia de Buenos Aires (CIC), República Argentina for financial support. They are indebted to the Facultad de Ciencias Exactas, Universidad Nacional de La Plata, República Argentina for financial support. M.F.E. would like to express his gratitude to Holger Pernice, Plácido García, Mike Finze, Stefan Balters, and Stefan von Ahsen for their friendship and valuable help in the laboratory work during his stay in Duisburg. This work is part of the PhD thesis of M.F.E. M.F.E. is a fellow of CONICET. C.O.D.V. is a member of the Carrera del Investigador of CONICET, República Argentina.

Supporting Information Available: Listing of atomic coordinates and equivalent isotropic displacement coefficients (Table IS) and anisotropic displacement parameters ($\text{\AA}^2 \times 10^3$) (Table IIS) for $\text{ClC}(\text{O})\text{OCF}_3$. This material is available free of charge via the Internet at <http://pubs.acs.org>.

References and Notes

- (1) Anderson, B. C.; Morlock, G. R. U.S. Patent 3,226,418; *Chem. Abstr.* **1966**, 64, 9598.
- (2) Aymonino, P. J. *Chem. Commun.* **1965**, 241.
- (3) Young, D. E.; Anderson, L. R.; Gould, D. E.; Fox, W. B. *Tetrahedron Lett.* **1969**, 9, 723.
- (4) Schack, D. J.; Maya, W. *J. Am. Chem. Soc.* **1968**, 91, 2902.
- (5) Gould, D. E.; Anderson, L. R.; Fox, W. B. U. S. Patent 3,769,312. *Chem. Abstr.* **1973**, 72, 54743.
- (6) Hermann, A.; Trautner, F.; Gholivand, K.; von Ahsen, S.; Varetti, E. L.; Della Védova, C. O.; Willner, H.; Oberhammer, H. *Inorg. Chem.* **2001**, 40, 3979.
- (7) (a) Cutin, E. H.; Della Védova, C. O.; Aymonino, P. J. *An. Asoc. Quím. Argent.* **1985**, 73, 171. (b) Varetti, E. L.; Aymonino, P. J. *J. Mol. Struct.* **1967–1968**, 1, 39. (c) Johnston, T.; Heicklen, J.; Stuckey, W. *Can. J. Chem.* **1968**, 46, 32.
- (8) (a) dos Santos Alonso, M.; Romano, R. M.; Della Védova, C. O.; Czarnowski, J. *Phys. Chem. Chem. Phys.* **2000**, 2, 1393. (b) Meller, R.; Moortgat, G. K. *Int. J. Chem. Kinet.* **1997**, 29, 579.
- (9) Chistensen, L. K.; Wallington, T. J.; Guschin, A.; Hurley, M. D. *J. Phys. Chem. A* **1999**, 103, 4202.
- (10) Wallington, T. J.; Schneider, W. F.; Sehested, J.; Bilde, M.; Nielsen, O. J.; Christensen, L. K.; Molina, M. J.; Molina, L. T.; Wooldridge, P. W. *J. Phys. Chem. A* **1997**, 101, 8264.
- (11) Gould, D. E.; Anderson, L. R.; Young, D. E.; Fox, W. B. *Chem. Commun.* **1968**, 1564.
- (12) Saunders: J. H.; Slocombe, R. J.; Hardy, E. E. *J. Am. Chem. Soc.* **1949**, 71, 752.
- (13) Gombler, W.; Willner, H. *J. Phys. E* **1987**, 20, 1286.
- (14) Argüello, G. A.; Grothe, H.; Kronberg, M.; Mack, H.-G. *J. Phys. Chem.* **1995**, 99, 17525.
- (15) Oberhammer, H. *Molecular Structure by Diffraction Methods*; The Chemical Society: London, 1976; Vol. 4, p 24.
- (16) Oberhammer, H.; Gombler, W.; Willner, H. *J. Mol. Struct.* **1981**, 70, 273.
- (17) Brodalla, D.; Mootz, D.; Boese, R.; Osswald, W. *J. Appl. Crystallogr.* **1985**, 18, 316.
- (18) Boese, R.; Nussbaumer, M. In *Situ Crystallisation Techniques*. In *Organic Crystal Chemistry*; Jones, D. W., Ed.; Oxford University Press: Oxford, U.K., 1994; pp 20–37.
- (19) *SHELTX-Plus Version SGI IRIS Indigo, a Complex Software Package for Solving, Refining and Displaying Crystal Structures*; Siemens: Germany, 1991.
- (20) Frisch, M. J.; Trucks, G. W.; Schlegel, H. B.; Scuseria, G. E.; Robb, M. A.; Cheeseman, J. R.; Zakrzewski, V. G.; Montgomery, J. A., Jr.; Stratmann, R. E.; Burant, J. C.; Dapprich, S.; Millam, J. M.; Daniels, A. D.; Kudin, K. N.; Strain, M. C.; Farkas, O.; Tomasi, J.; Barone, V.; Cossi, M.; Cammi, R.; Mennucci, B.; Pomelli, C.; Adamo, C.; Clifford, S.; Ochterski, J.; Petersson, G. A.; Ayala, P. Y.; Cui, Q.; Morokuma, K.; Malick, D. K.; Rabuck, A. D.; Raghavachari, K.; Foresman, J. B.; Cioslowski, J.; Ortiz, J. V.; Stefanov, B. B.; Liu, G.; Liashenko, A.; Piskorz, P.; Komaromi, I.; Gomperts, R.; Martin, R. L.; Fox, D. J.; Keith, T.; Al-Laham, M. A.; Peng, C. Y.; Nanayakkara, A.; Gonzalez, C.; Challacombe, M.; Gill, P. M. W.; Johnson, B. G.; Chen, W.; Wong, M. W.; Andres, J. L.; Head-Gordon, M.; Replogle, E. S.; Pople, J. A. *Gaussian 98*, revision A.7; Gaussian, Inc.: Pittsburgh, PA, 1998.
- (21) Kohn, W.; Sham, L. *J. Phys. Rev. A* **1965**, 140, 1133.
- (22) Becke, A. D. *J. Chem. Phys.* **1993**, 98, 5648.
- (23) Becke, A. D. *J. Chem. Phys.* **1993**, 98, 1372.
- (24) Lee, C.; Yang, W.; Parr, R. G. *Phys. Rev. B Condens. Matter* **1988**, 41, 785.
- (25) Møller, C.; Plesset, M. S. *Phys. Rev.* **1934**, 46, 618.
- (26) Argüello, G. A.; Willner, H.; Malanca, F. E. *Inorg. Chem.* **2000**, 39, 1195.
- (27) Katon, J. E.; Griffing, M. G. *J. Chem. Phys.* **1973**, 59, 5868.
- (28) Nyquist, R. A. *Spectrochim. Acta A* **1972**, 28, 285.
- (29) (a) Varetti, E. L.; Aymonino, P. J. *J. Mol. Struct.* **1967–1968**, 1, 39. (b) Cutin, E. H.; Della Védova, C. O.; Aymonino, P. J. *An. Asoc. Quím. Argent.* **1985**, 73, 171.
- (30) Mack, H.-G.; Oberhammer, H.; Della Védova, C. O. *J. Phys. Chem.* **1991**, 95, 4238.
- (31) Hughes, E. D.; Ingold, C. K.; Whitfield, I. C. *Nature*, **1941**, 147, 206.
- (32) Lewis, E. S.; Herndon, W. C. *J. Am. Chem. Soc.* **1961**, 83, 1955.
- (33) Ramsberger, H. C.; Waddington, G. *J. Am. Chem. Soc.* **1948**, 55, 214.
- (34) Sipachev, V. A. *J. Mol. Struct.* **2001**, 567/568, 67.
- (35) Gobbato, K. I.; Leibold, C.; Centeno, S.; Della Védova, C. O.; Mack, H.-G.; Oberhammer, H. *J. Mol. Struct.* **1996**, 380, 55.
- (36) Nagy, P. I.; Smith, D. A.; Alagona, G.; Ghio, C. *J. Phys. Chem.* **1994**, 98, 486. The binding energy is expressed by the equation $\Delta E^c = \Delta E - \text{BSSE} + \text{GEOM}$ where ΔE^c and ΔE are the corrected and uncorrected binding energies, respectively, BSSE corresponds to the error due to the basis set superposition, and the term GEOM takes into account the geometry differences between free monomers and each of the subunits as they occur in the complex dimer. These terms can be calculated through equations $\Delta E = E(\text{AB}) - E^{m,m}(\text{A}) - E^{m,m}(\text{B})$, $\text{BSSE}_{(\text{d},\text{d}-\text{d},\text{m})} = E^{\text{d},\text{d}}(\text{A}) - E^{\text{d},\text{m}}(\text{A}) + E^{\text{d},\text{d}}(\text{B}) - E^{\text{d},\text{m}}(\text{B})$, and $\text{GEOM}_{(\text{d},\text{m}-\text{m},\text{m})} = E^{\text{d},\text{m}}(\text{A}) - E^{m,m}(\text{A}) + E^{\text{d},\text{m}}(\text{B}) - E^{m,m}(\text{B})$ where the superscripts m and d refer to the monomers and dimer, respectively. The first superscript refers to the geometry of the species and the second one refers to the basis set used to calculate the energy at a geometry defined by the first superscript. The terms BSSE have been calculated by applying the counterpoise procedure developed by Boys and Benardi.³⁷
- (37) Boys, S. F.; Benardi, F. *Mol. Phys.* **1970**, 19, 553.
- (38) Durig, J. R.; Griffin, M. G. *J. Mol. Spectrosc.* **1977**, 64, 252.
- (39) (a) NBO, version 3.1; Glendening, E. D.; Reed, A. E.; Carpenter, J. E.; Weinhold, F. (b) Carpenter, J. E.; Weinhold, F. *J. Mol. Struct. THEOCHEM* **1988**, 169, 41.
- (40) Gobbato, K. I.; Mack, H.-G.; Oberhammer, H.; Ulic, S. E.; Della Védova, C. O.; Willner, H. *J. Phys. Chem. A* **1997**, 101, 2173.